Polish J. Chem., **78**, 1811–1822 (2004)

Potential and Strain Rate Impact on the Electrochemical Properties of 304L Stainless Steel Under Tensile Stresses*

by K. Darowicki, J. Orlikowski, A. Arutunow*****

Department of Electrochemistry, Corrosion and Materials Engineering,
Gdansk University of Technology, PL - 80-952 Gdansk, 11/12 Narutowicza Str., Poland

(Received June 2nd, 2004; revised manuscript July 12th, 2004)

The majority of this work was to find out if Dynamic Electrochemical Impedance Spectroscopy can be applied for non-stationary electrochemical processes examination, such as the instantaneous changes during the passive layer cracking. Characterization of the passive layer cracking dynamics is very important from the diagnostics point of view. Especially, if investigated materials are protected by passive films exposed to substantial loads. Presented paper proves that the Dynamic Electrochemical Impedance Spectroscopy allows the determination of instantaneous impedance changes during the initiation stage of the SCC process, which is related to the crack of passive layer. Moreover, mentioned procedure makes possible prediction of the passive layer rupture under tensile stresses. Instantaneous impedance spectra for 304L stainless steel specimens in 0.5 M NaCl solution at room temperature were recorded. Measurements were conducted for different potential values and various strain rates according to the double-factor impact – electrochemical and mechanical. Impedance spectra have been depicted in the 3D diagrams illustrating system's impedance evolution over time. Each spectrum refers to 0.6 second of process duration, so reflecting the changes in the investigated system dynamics.

Key words: passive layer properties, passive layer cracking, DEIS, 304L stainless steel, tensile stresses

Rupture of the passive layer under tensile stresses leads to the stress corrosion cracking (SCC) in many cases, which is one of the most dangerous kinds of corrosion damages because material failure is often very rapid and unexpected. It is connected with a combination of stresses, material structure, and an aggressive electrolyte environment [1,2]. Two stages of the SCC can be distinguished: the initiation and the crack propagation stage. The former is often more essential for the time to failure. Miscellaneous models have been proposed for the initiation stage of the SCC. Disruption of the protective surface film (passive film) is the most common attribute of each model in order to expose bare metal to the aggressive electrolyte environment. Both chemical and mechanical processes have been postulated as the reason for this rupture. For instance, researches under different material/environment combinations at room or elevated temperatures were oriented towards the SCC nucleation

* Dedicated to Prof. Dr. Z. Galus on the occasion of his 70th birthday.

** ISE Member

*** Corresponding author e-mail: anka@chem.pg.gda.pl

in terms of pitting [3–5], film rupture [6], anodic dissolution [7], and hydrogen embrittlement [7]. Newman [1] characterized five electrochemical conditions, which may bring to the SCC in electrolytes presumed that the material has a susceptible metallurgy. Works, which focused on fatigue corrosion point out that inclusions are also potential starting sites for crack [8,9].

Electrochemical impedance spectroscopy has been applied for many years to investigate different electrochemical processes and now is recognized as one of the most powerful studying methods for corrosion detection. Classical EIS can give some information about the SCC processes, but only before and just after the moment of cracking that is in a stable state [10–12]. Impedance measurements of the active-passive transition, investigation of the stress corrosion at constant strain rate, and for different strain rates were carried out in order to verify the use of this technique. The application of impedance technique to the SCC by Oltra and Keddam was presented [13]. However, classical impedance measurements require linearization, stability and causality conditions [10,11]. A novel Dynamic Electrochemical Impedance Spectroscopy elaborated in the Department of Electrochemistry, Corrosion and Materials Science of Gdansk University of Technology gives possibility of determination the impedance characteristics in time domain during rupture of the protective passive layer. This fact is connected with the analysing methodology, which enables the selective time – frequency analysis of measurement data. More information about the passive layer cracking dynamics obtained by this method can develop SCC monitoring in the future.

EXPERIMENTAL

Impedance measurements were carried out under different potential and strain rate conditions. Examined samples were made of 304L stainless steel in the form of bars. The composition of 304L stainless steel (SS) is given below in Table 1.

Table 1. Normalized chemical composition of AISI 304L SS (average values).

C	Mn	Si	P	S	Cr	Ni	Fe
≤ 0.03%	≤ 2.0%	≤ 1.0%	≤ 0.04%	≤ 0.03%	17–19%	9–11%	Bal.

Samples were mounted in a measurement cell and then in a tensile testing machine INSTRON 8503. Silver/silver chloride electrode was used as a reference electrode, and the auxiliary electrode was made of platinum net. Characteristic dimensions of a specimen and the measurement cell are presented in Figure 1.

Researches were performed in 0.5 M NaCl solution at ambient temperature. Time of impedance measurement was correlated with tensile process. Total time of a single performed measurement was equal to 320 seconds. Maximum elongation was equal to about 12 mm for each sample investigated. The measurement set-up consisted of an ELPAN EP20A potentiostat and a National Instruments AT-MIO-16E-1 card generating the perturbation signal. Impedance measurements were conducted for the frequency range: 2640 Hz – 12 Hz. The amplitudes of all elementary sinusoidal signals were equal to $u_0 = 8$ mV. Voltage perturbation and current response signals were registered by two National Instruments PCI-6052E cards driven by one signal. The sampling frequency was equal to 12288 Hz and the multi sinusoidal signal of 12 sinusoids was utilized.

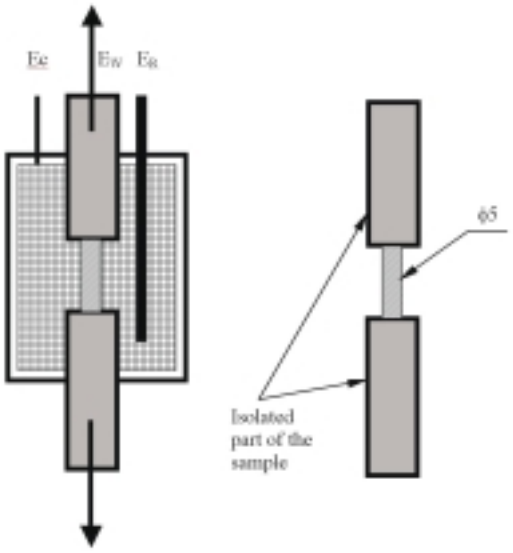

Figure 1. Measurement cell and characteristic dimension of examined samples.

RESULTS AND DISCUSSION

Detailed analysis of investigated process was based on the initial range of obtained tensile curves, which reflects transition from elastic into plastic region. Dependence between stresses and relative elongation is presented in Figure 2.

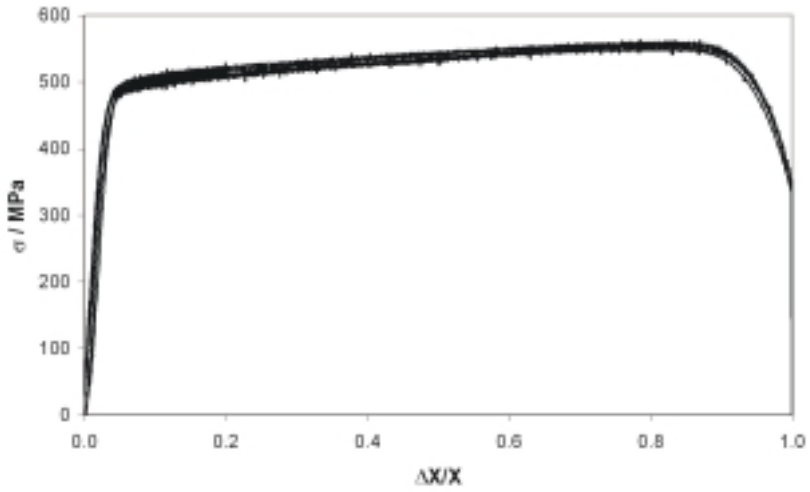

Figure 2. Stresses as a function of elongation for 304L stainless steel.

Straight line indicates the elongation of 12% (relative elongation $\Delta x/x = 0.12$) and so limiting elongation range that can be found in all diagrams illustrated in this paper. It should be noted that $\Delta x/x = 0.12$ reflects the initial 40 seconds of a single measurement. Time of a single measurement was too short, so mechanical properties of examined material could not change considerably with potential. Any curve changes with potential cannot be seen. As a result the tensile strength takes an average value of 562 MPa and does not depend on the potential.

Figures 3 (a–e) show impedance spectra as a function of relative elongation for different potential values. Respectively, each spectrum relates to the measurement time of 0.6 second. The effect of potential on the system's impedance is obvious. More important is that these impedance spectra illustrate very distinct passive – active transition state according to the applied potential. Impedance decrease depends

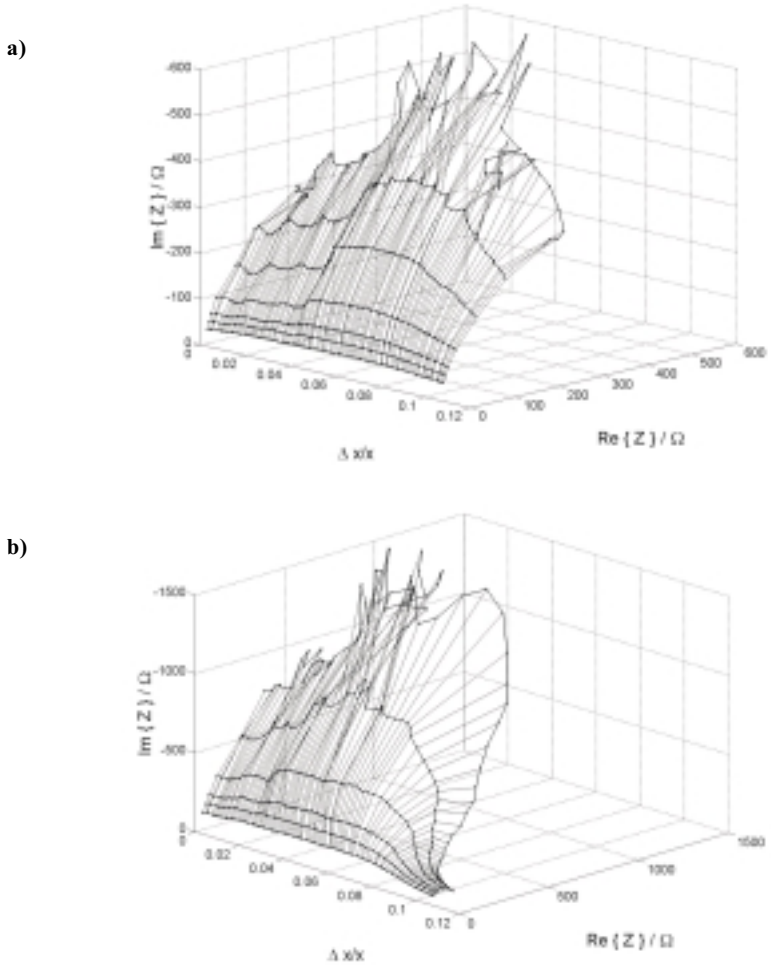

Figure 3. Instantaneous impedance spectra of the passive-active transition *versus* relative elongation: a) E = –0.150 V, b) E = –0.100 V, c) E = –0.050 V, d) E = +0.050 V, e) E = +0.150 V.

c)

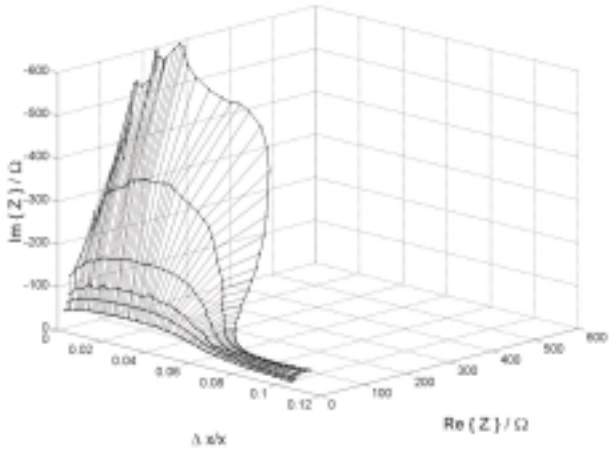

d)

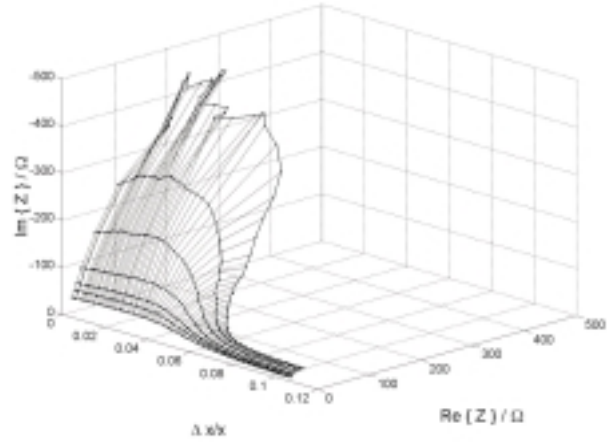

e)

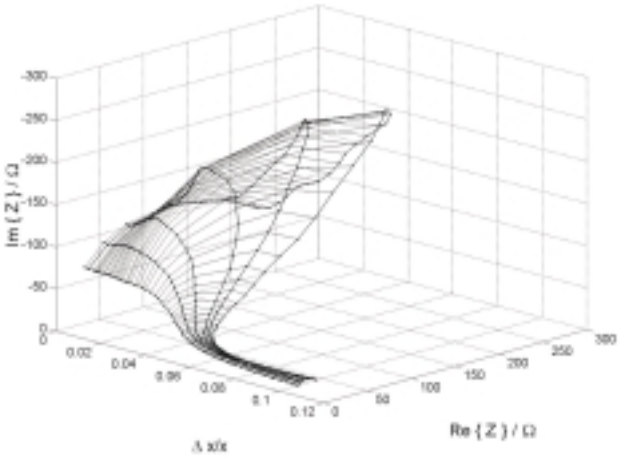

Figure 3 (continuation)

strongly on the potential, *e.g.* decreases more quickly with potential values increasing in anodic direction at the same time. For the corrosion potential of –0.150 V one can see slight decrease in impedance values. Spectra are observed rather in the form of straight lines and have diffusion character that means they exhibit the passive state. Some changes in the spectra form can be found for the potential of –0.100 V. In this case impedance takes the maximum value of 1500 Ω. With potential values growing up one can observe more visible changes in impedance spectra, so that the passive – active transition becomes clearer. Finally, for the highest potential of +0.150 V impedance takes the minimum value of 100 Ω.

Figures 4 (a–e) depict impedance spectra in the form of Nyquist plots *versus* relative elongation for investigated range of strain rates. Presented spectra have a dynamic character of changes in relation to the relative elongation. Occurrence of two

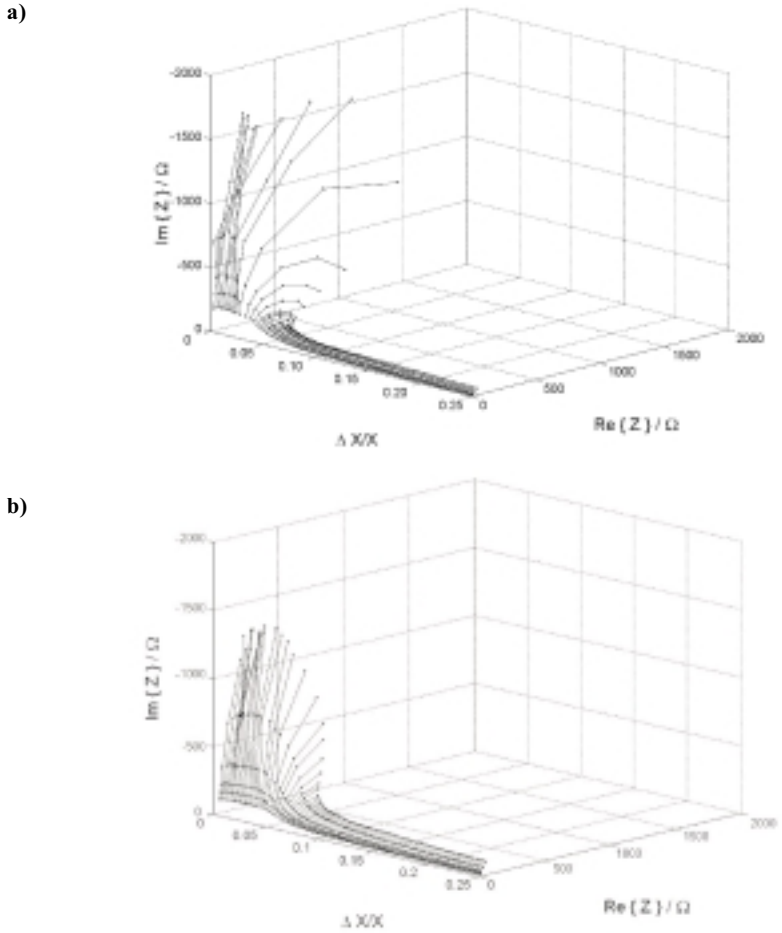

Figure 4. Instantaneous impedance spectra of the passive-active transition *versus* relative elongation for different strain rates (E = 0.000 V): a) $1.04 \cdot 10^{-5}$ m/s, b) $2.08 \cdot 10^{-5}$ m/s, c) $4.17 \cdot 10^{-5}$ m/s, d) $8.33 \cdot 10^{-5}$ m/s, e) $16.67 \cdot 10^{-5}$ m/s.

c)

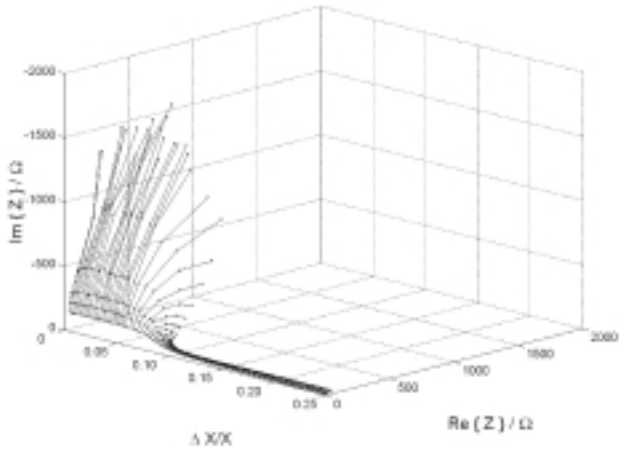

d)

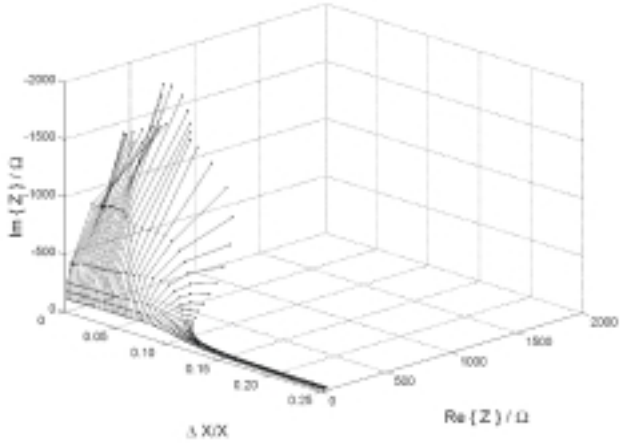

e)

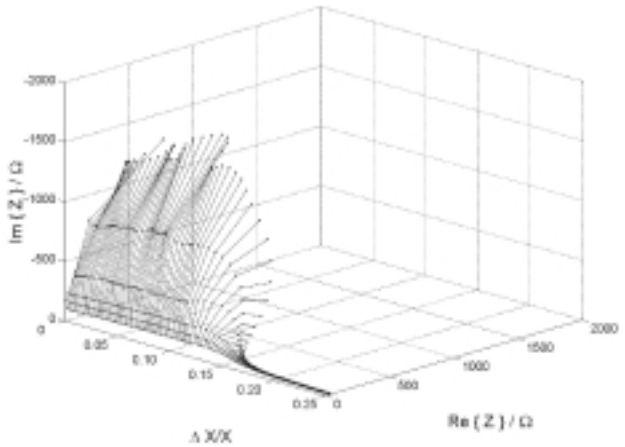

Figure 4 (continuation)

regions on each spectrogram can be easily found: first referring to the stable state (impedance spectra in the form of vertical lines) and another related to the active state (impedance spectra in the form of semicircles). Transition from the stable into the active region was due to the passive layer cracking process. Upon the analysis of impedance spectra the character of changes can be seen according to applied strain rates. It is clearly visible that the moment of the passive layer cracking depends on the strain rate value: for the lowest strain rates process of the passive layer rupture goes under the lowest elongation values. So the higher strain rate had been applied the longer time was needed to breakdown the passive layer. Increase in strain rate values implies the relative elongation values for which the passive layer cracking can be observed (impedance grows less distinctly together with changes in the shape of impedance spectra). The fact that the higher strain rate had been applied the longer time was needed to breakdown the passive layer can be accounted for the fact that slip planes are formed for faster strain processes [14,15]. Moreover, structure is strengthening by martensit phase that appears during the tensile process [14,16].

Additionally, exemplary fitting of presented impedance spectra is depicted in Figure 5. Analysis of recorded impedance spectra had to be performed to execute detailed characterization of processes occurring during the tensile tests. Therefore, for the potential 0.000 V equivalent circuit presented in Figure 6 can describe process run.

Changes of electrochemical parameters as a function of relative elongation could be seen in Figures 7–9. Strong influence of the applied strain rates can be seen. One can also find the correlation between the spectra presented in Figure 4 and changes of electrochemical parameters in Figures 7–9. Both experience a change at the same instants of time.

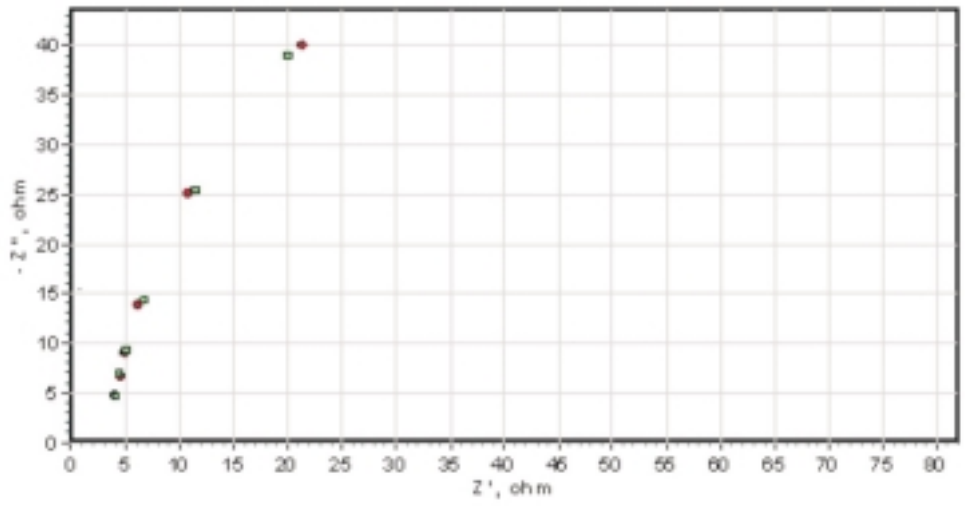

Figure 5. Fitting results for the proposed equivalent circuit for an exemplary spectrum: (–○–) – fitting points to experimental results; (–□–) – experimental results.

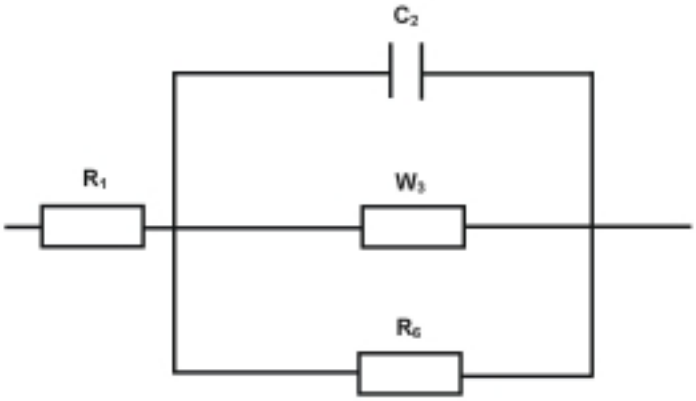

Figure 6. Equivalent circuit: R_1 – electrolyte resistance, C_2 – capacitance of amorphous part of the passive layer, W_3 – Warburg coefficient of amorphous part of the passive layer, R_6 – charge transfer resistance.

The R_6 parameter changes with relative elongation are illustrated in Figure 7 for examined strain rates. This parameter characterizes the charge transfer resistance connected with electrochemical processes that take place on the electrode's surface. High R_6 values are responsible for occurrence of durable passive film. On the other hand, decrease in R_6 values can denote the cracking process or tightness decay of passive layer, hereby initiates corrosion processes. Phenomenon described in Figure 3 can be confirmed on the basis of the analysis observed in Figure 7. For each strain rate examined one can see distinct drop of R_6 values with relative elongation. Thus, it can

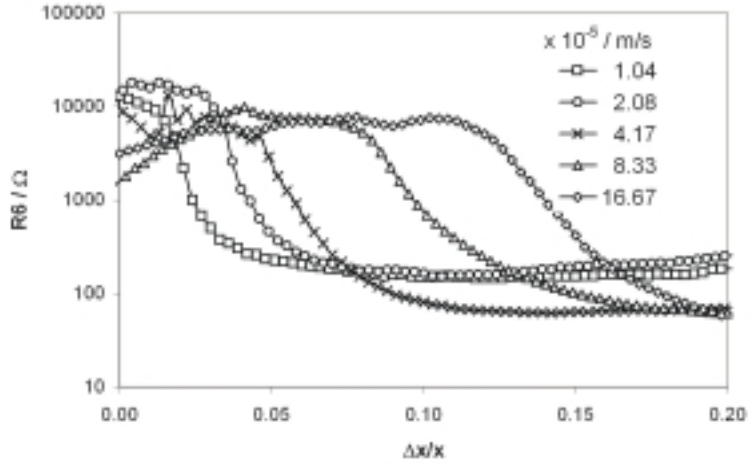

Figure 7. Relative elongation dependence of charge transfer resistance (R_6): (–□–) $1.04 \cdot 10^{-5}$ m/s, (–○–) $2.08 \cdot 10^{-5}$ m/s, (–X–) $4.17 \cdot 10^{-5}$ m/s, (–△–) $8.33 \cdot 10^{-5}$ m/s, (–◇–) $16.67 \cdot 10^{-5}$ m/s.

be stated that process of the passive layer cracking was detected for all investigated strain rates. Threshold elongation reflected the decay of passive film tightness depends on the strain rate parameter.

Besides the charge transfer resistance R_6, another electrochemical parameter that allows the determination of electrochemical conditions occurring on the electrode's surface subjected to electrochemical investigations is capacitance (C_2) of the passive layer. Dependence between C_2 and relative elongation is depicted in Figure 8 for different strain rates. In accordance with used equivalent circuit C_2 parameter is involved with the passive layer capacitance and the capacitance of electric double layer. Though, the differentiation of particular capacitances is not possible due to limited range of applied frequencies, trend changes designation of this parameter allows to conclude what is the course of changes of electrochemical processes during tensile process. The passive layer cracking process leads to increase in the capacitance of passive layer, and corrosion processes progress causes that the capacitance of electric double layer grows up. Described capacitance increase can be seen in Figure 8 distinctly. The relative elongation value for which this increase starts strongly depends on the strain rate applied.

Figure 9 represents changes of Warburg coefficient W_3 as a function of relative elongation for different strain rates. Warburg coefficient is involved with diffusion processes, so when this parameter grows less diffusion processes are limited. During the passive layer cracking or when the passive layer tightness decay diffusion decrement occurs. For low values of relative elongation, W_3 reaches similar values for each strain rate (initial conditions are the same for each sample examined).

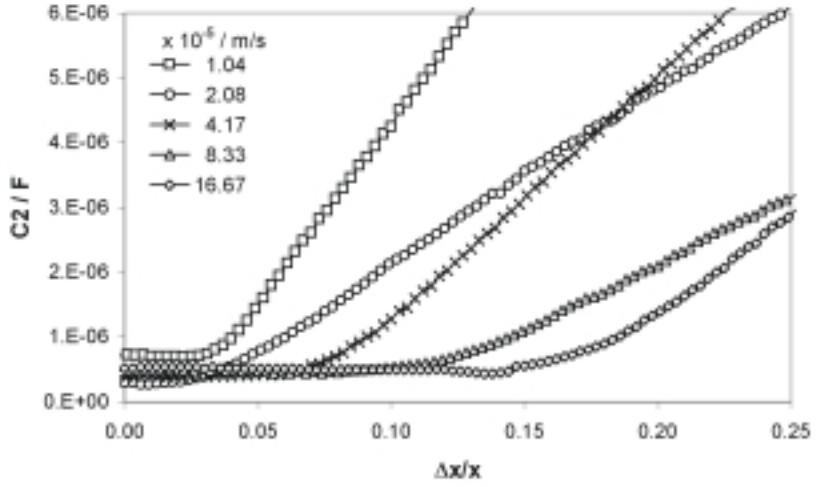

Figure 8. Relative elongation dependence of capacitance of amorphous part of the passive layer (C_2): (–□–) $1.04 \cdot 10^{-5}$ m/s, (–○–) $2.08 \cdot 10^{-5}$ m/s, (–X–) $4.17 \cdot 10^{-5}$ m/s, (–△–) $8.33 \cdot 10^{-5}$ m/s, (–◇–) $16.67 \cdot 10^{-5}$ m/s.

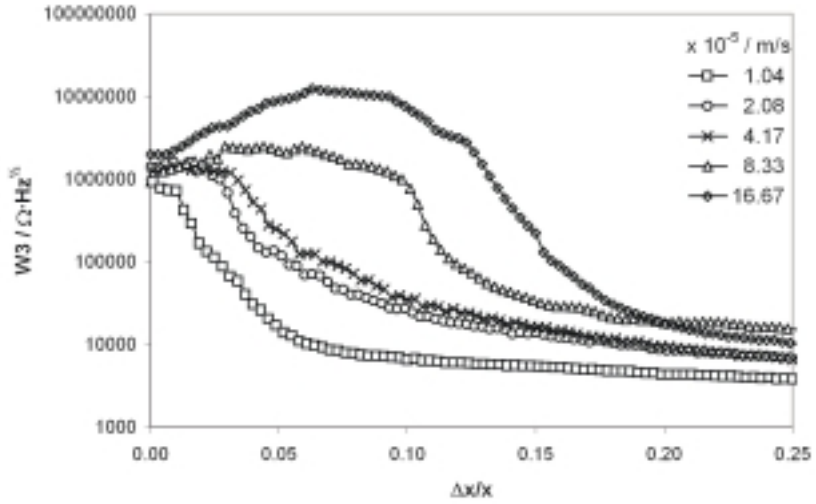

Figure 9. Relative elongation dependence of Warburg coefficient of amorphous part of the passive layer (W_3): (–□–) $1.04 \cdot 10^{-5}$ m/s, (–○–) $2.08 \cdot 10^{-5}$ m/s, (–X–) $4.17 \cdot 10^{-5}$ m/s, (–△–) $8.33 \cdot 10^{-5}$ m/s, (–◇–) $16.67 \cdot 10^{-5}$ m/s.

Decreases in W_3 values with relative elongation are also noticeable. Distinct changes depend on the sample's strain rate. The W_3 decrement for the highest strain rates occurs for high relative elongation values, whereas with the decrease in strain rate values the relative elongation for which passive layer tightness deteriorates also is diminished. It is well correlated with trends observed for R_6 and C_2 parameters. The highest W_3 values reflecting the tightest passive layer are observed for the highest strain rates. Such situation can be seen up to $\Delta x/x = 0.25$. In comparison to R_6 and C_2 Warburg coefficient represents tensile strength of the passive layer. Changes involved with the rate of repassivation processes are slightly visible for higher relative elongation values.

CONCLUSIONS

The investigated SCC initiation stage, *i.e*. the passive layer cracking, caused by tensile stresses can be described as a very fast electrochemical process.

Presented results are the first to take into consideration the dynamic changes during the passive layer cracking and prove that application of Dynamic Electrochemical Impedance Spectroscopy can be a very useful tool in further prediction of the SCC initiation process in comparison to classical impedance techniques.

The transition range from passive into active state during the passive layer cracking process was successfully detected.

The effect of potential and strain rate on the system's dynamics is significant. Although, fast detection of the passive layer cracking with the rupture of investigated samples cannot be identified.

Increase in potential values in the anodic direction diminishes system's impedance distinctly.

Moment of the passive layer rupture depends strongly on the applied strain rate. It takes more time to breakdown the layer when higher strain rate is employed.

Rapid dynamics of electrochemical processes, such as the passive layer cracking, for which single measurement is of 0.6 second, precludes application of additional microscopic techniques.

REFERENCES

1. Newman R.C., Stress-Corrosion Cracking Mechanisms: in (Eds.) P. Marcus and J. Oudar, Corrosion Mechanisms in Theory and Practice, Marcel Dekker, Inc., New York, 1995, pp. 309–372.
2. Suter T., Webb E.G., Bohni H. and Alkire R.C., *J. Electrochem. Soc.,* **148,** B174 (2001).
3. Christman T.K., *Corrosion*, **46,** 450 (1990).
4. Ashour E.A., Abd El Meguid E.A. and Ateya B.G., *Corrosion*, **53,** 450 (1997).
5. Isaacs H.S., *J. Electrochem. Soc.,* **135,** 2180 (1988).
6. McEvily A.J. and Bond A.P., *J. Electrochem. Soc.,* **112,** 112 (1965).
7. Rhodes P.R., *Corrosion*, **25,** 462 (1969).
8. Cottis R.A. and Husain Z., *Met. Technol.,* **9,** 104 (1982).
9. Shalby H.M., Begeley J.A. and Macdonald D.D., *Corrosion*, **52,** 262 (1996).
10. Gabrielli C., Identification of electrochemical processes by frequency response analysis, Technical Report Number 004/83, Farenborough 1995.
11. Macdonald D.D., Application of Electrochemical Impedance Spectroscopy in Electrochemistry and Corrosion Science: in (Eds.) R. Varma and J.R. Selman, Techniques for Characterization of Electrodes and Electrochemical Processes, John Wiley & Sons, Inc., New York, 1991, pp. 515–647.
12. Ross J. Macdonald and Johnson W.B., Fundamentals of Impedance Spectroscopy, in (Ed.), J. Ross Macdonald Impedance Spectroscopy: Emphasizing Solid Materials and Systems, John Wiley & Sons, Inc., New York, 1987, pp. 1–20.
13. Oltra R. and Keddam M., *Corros. Sci.,* **28,** 1 (1988).
14. Lee W.S. and Lin C.F., *Mat. Sci. Eng.,* **A 308,** 124 (2001).
15. Mateo A., Llanes L., Iturgoyen L. and Anglada M., *Acta Mater.,* **44,** 1143 (1996).
16. Lee W.S. and Lin C.F., *Scripta Mater.,* **43,** 777 (2000).